Dynamic LiFi Attocellular Networks Slicing for 5G Services

Hamada Alshaer and Harald Haas
LiFi R&D centre, Technology & Innovation Centre
The University of Strathclyde, UK
{h.alshaer,harald.haas}@strath.ac.uk

***Abstract*—A multi-service light fidelity (LiFi) attocellular network should be resource engineered to efficiently support fifth generation (5G) services on customized network slices. Mobile virtual network operators (MVNOs) request network slices to offer customized services according to their service level agreement (SLA) constraints in terms of resource guarantees or data rate targets. However, there are two main challenges to meet these network resource and services slicing guarantees in a sliced LiFi attocellular network: i) conflicting services requirements and ii) dynamic resource quota allocation to slices. A multi-policy resource scheduler is developed to support dynamic LiFi network slicing based on network resource and service utility optimization. The scheduler runs on a utility-based heuristic scheduling algorithm, which can simultaneously support multiple MVNOs to offer delay and throughput sensitive services on different LiFi network slices. This enables MVNOs to deploy their network slice quota customization policies that support different traffic profiles and specific-slice service management policies. The obtained results demonstrate that the weights of utility functions can be adjusted automatically according to the LiFi AP channel conditions and the SLA constraints of MVNOs.**

***Index Terms*—LiFi network slicing, utility scheduler, network slices, QoS .**

I. Introduction

Spectrum resources in light fidelity (LiFi) attocellular networks are massive. This circumstance can be used to efficiently augment the fifth generation (5G) services, namely: ultra-reliable low-latency communication (URLLC), enhanced mobile broad band (eMBB), and massive machine type communication (mMTC) services [1]. These services are sensitive to various quality-of-service (QoS) parameters, particularly throughput and delay. LiFi mobile network operators (MNOs) require to offer network-as-a-service to mobile virtual network operators (MVNOs) in the form of network slices, which are configured on resource quotas allocated to each LiFi network attocell [2]–[4]. A service level agreement (SLA) is established between MVNOs and a MNO, which specifies the QoS requirements and the quota constraints of their leased network slices in terms of minimum and maximum network resource guarantees or aggregate data rate targets [5], [6]. Utility functions map the constraints of QoS metrics to utility values, which can support more flexible dynamic resource scheduling and allocation to users. They can also provide MVNOs with resource and network parameters to customize and prioritize their slice performance metrics according to the service requirements and network conditions [7]. This paper develops resource utility-based wireless spectrum scheduling policies for dynamically slicing LiFi attocellular networks, as shown in Fig.1. A medium access control (MAC) packet scheduler runs based on the proposed resource and service utility-based scheduling policies to manage the resource quotas allocated to the different network slices in the attocells. The scheduling policies achieve different objectives, specifically meeting the delay and throughput requirements of users while maximizing the network slices utility [2], [8].

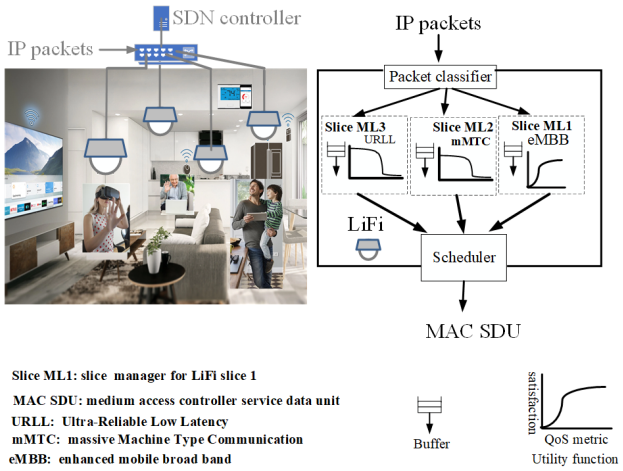

Fig. 1: SDN-enabled multi-tenant LiFi attocellular network

In [9], a fast heuristic algorithm was developed to share the physical resource blocks (PRBs) of a three-cell LTE network among three service providers (SPs). It aims to maximize the network sum rate and guarantee a minimum target data rate for each SP. However, it does not guarantee inter-slice isolation and ensure rate control on the target data rate of slices with users that have good channel conditions. In [10] the authors formulated a utility-based dynamic resource allocation (DRA) optimization problem, which aims to maximize the number of satisfied users receiving real-time and non-real time services in a single LTE base station. However, their proposed sigmoidal and marginal utility functions based on Eqs. (9,10) in [10] run with wide ranges of delay and throughput, which make them impractical in matching the delay and throughput requirements of small cell network slices. In [7] a utility-based transport layer scheduling approach was developed to

This is a peer-reviewed, accepted author manuscript of the following article: Alshaer, H., & Haas, H. (2022). Dynamic LiFi attocellular networks slicing for 5G services. In ICC 2022 - IEEE International Conference on Communications (pp. 583-588). IEEE. https://doi.org/10.1109/ICC45855.2022.9839152

slice a single 5G new radio (5GNR) cell. A cell slice is abstracted with a buffer; and its constraints are defined based on the traffic load and service type. The throughput and delay utility function are based on the buffer model and service traffic requirements. CellSlice [11] improves the single base station network virtualization substrate (NVS) [8] by slicing the network gateway, where the downlink and uplink traffic is shaped according to their network slice constraints.

In contrast to the above, this paper develops, for the first time, a cross-layer network scheduler to support LiFi attocellular networks slicing. A network slice buffer in each LiFi AP attocell [7], [12], is handled by a slice software agent manager. The software agents running in the LiFi APs are characterized by utility functions designed to translate the QoS metrics (i.e., delay and throughput) to network resource utility values. Multiple utility-based scheduling policies are developed to dynamically allocate the LiFi downlink channel resources of LiFi APs to the network slices according to their users' service utility and SLA constraints, as shown in Fig. 1.

The rest of this paper is structured as follows. Section II explains the network system model. Section III states the optimization problem objective and explains its constraints. Section IV defines the utility function models and scheduling policies. Section V explains the proposed heuristic utility-based scheduling algorithm. Section VI discusses the performance of utility-based scheduling policies. Section VII concludes the paper and presents key findings.

II. System model

The system model is a LiFi attocellular network composed of a set of LiFi APs, $\mathcal{A} = \{1, 2, \cdots, |\mathcal{A}|\}$, which is run by a single MNO. The network is resource sliced into a set of network slices, $\mathcal{S} = \{1, 2, \cdots, |\mathcal{S}|\}$. A network slice supports a single service offered by a single MVNO (tenant). So, $s \in \mathcal{S}$ refers also to the index number of MVNO. Network slices are allocated resource quotas to LiFi attocells, where they are instantiated. An attocell AP has a maximum transmit power, $p_{a,\max}$, $\forall a \in \mathcal{A}$. The AP downlink channel bandwidth is divided into set of Direct Current-biased Optical Orthogonal Frequency-Division Multiplexing (DCO-OFDM) sub-carriers (resource units), $\mathcal{N} = \{1, 2, \cdots, |\mathcal{N}|\}$, which each has a bandwidth b Hz. A resource unit n at sub-frame t in attocell a is described by a tuple $[a, t, n]$ [9]. A LiFi AP uses half of the available sub-carriers to realize the Hermitian conjugate of the complex-valued symbol after modulation, as only real-valued signals can be transmitted to users [13]. The LiFi AP downlink channel is managed by the orthogonal frequency-division multiple access protocol (OFDMA) [2], [14]. A user is connected to a single AP offering the best signal strength. The transmission time on the LiFi downlink channel is divided into scheduling time intervals, with each corresponding to a sub-frame of duration 1 ms. The software-defined networking (SDN) controller updates the state of resources in each LiFi attocell every sub-window of duration T sub-frames. It is assumed that all the LiFi APs receive perfect channel gain information from the users under their coverage. A channel gain of user k subscribed to MVNO s and assigned a resource unit $[a, t, n]$ is denoted by $h_{sk}^{[a,t,n]}$. A sub-carrier is subject to additive white Gaussian noise (AWGN) denoted by σ^2. The set of users associated to AP a and subscribed to MVNO s is denoted by $\mathcal{K}_s^a$. MVNOs have SLAs that define their minimum and maximum target rate guarantees in each LiFi attocell a, $R_{\min}^{a,s}$ and $R_{\max}^{a,s}$, respectively.

Dynamic LiFi attocellular network resources slicing among MVNOs is controlled by power allocation to sub-carriers and data rate achieved on each sub-carrier assigned to each user. The power allocation vector of all APs to sub-carrier n at sub-frame t is denoted by $\mathbf{p}_{[t,n]} = [p_{[1,t,n]}, \cdots, p_{[A,t,n]}]$. The signal-to-interference-plus-noise-ratio (SINR) for user $k \in K_s^a$ is calculated as follows [4]:

$$\text{SINR}_{sk}^{[a,t,n]} = \frac{p_{[a,t,n]}|h_{sk}^{[a,t,n]}|^2}{\sigma^2 + \sum_{j=1, j\neq a}^{A} p_{[j,t,n]}|h_{sk}^{[j,t,n]}|^2}. \quad (1)$$

Hence, the achievable data rate of $k \in \mathcal{K}_s^a$ is given by the Shannon theorem as follows:

$$\gamma_{sk}^{[a,t,n]} = \frac{b}{2}\log_2\left(1 + \text{SINR}_{sk}^{[a,t,n]}\right). \quad (2)$$

The data rate allocated to users depends on the allocated resource units and their achievable data rates. A decision variable $z_{sk}^{[a,t,n]}$ is required to ensure a unique resource allocation to a single user k associated to MVNO s per $[a, t, n]$, as given by:

$$z_{sk}^{[a,t,n]} = \begin{cases} 1, & \text{if resource } [a,t,n] \text{ is allocated to user } (s,k) \\ 0, & \text{if otherwise,} \end{cases} \quad (3)$$

When users achieve higher data rates on their allocated sub-carriers, they drive a higher utility from the network. The achievable data rate of MVNO s is the total data rate achieved by their subscribed users. A utility function maps the resulted network slice performance from the allocated network resources to each user subscribed to MVNO s, $\forall s \in S$, to network utility values. The network utility of MVNO s in the LiFi attocell a is denoted by $U_s^a(x_s^{[a,t,n]})$, where

$$x_s^{[a,t,n]} = \sum_{k\in\mathcal{K}_s^a}\sum_{t=1}^{T}\sum_{n=1}^{N} z_{sk}^{[a,t,n]}\gamma_{sk}^{[a,t,n]}, \quad \forall a, t, n. \quad (4)$$

The utility function is continuously differential, non-decreasing and concave to balance the efficiency and fairness of the resource allocation. The proposed scheduling algorithm aims to maximize the total weighed system utility, U_w, which is expressed as follows:

$$U_w = \sum_{a\in A}\sum_{s\in S}\omega_s^a U_s^a(x_s^{[a,t,n]}), \quad \forall t, n, \quad (5)$$

where ω_s^a is a slice-specific weight parameter which a MVNO can tune to customize their slice traffic scheduling per attocell a according to QoS priority metrics. The channel quality conditions impact the utility values each user can drive from their allocated network resources. Therefore, optimal scheduling uses utility functions that serve as an optimization objective for maximizing the data rate transmission of users, which maximizes the weighted sum of network slices utilities.

III. Problem Formulation

The optimization objective (6) is to find the resources $\mathbf{z}$ that maximizes the weighted sum of network slices utilities.

$$\max_{\mathbf{z}} \quad \sum_{a\in A}\sum_{s\in S}\omega_s^a U_s^a(x_s^{[a,t,n]}) \tag{6}$$

$$\text{s.t.} \quad \sum_{s=1}^{S}\sum_{k\in\mathcal{K}_s^a} z_{sk}^{a,t,n} \le 1, \quad \forall a,t,n \tag{7}$$

$$-\sum_{k\in\mathcal{K}_s^a}\sum_{t=1}^{T}\sum_{n=1}^{N} z_{sk}^{[a,t,n]}\gamma_{sk}^{[a,t,n]} \le -\gamma_{s,\min}^{a}, \quad \forall a,s \tag{8}$$

$$\sum_{k\in\mathcal{K}_s^a}\sum_{t=1}^{T}\sum_{n=1}^{N} z_{sk}^{[a,t,n]}\gamma_{sk}^{[a,t,n]} \le \gamma_{s,\max}^{a}, \quad \forall a,s \tag{9}$$

$$z_{sk}^{a,t,n} \in \{0,1\}, \quad \forall a,t,n,k,s \tag{10}$$

$$p_{a,t,n} \ge 0, \quad \forall n \tag{11}$$

Constraint (7) restricts user association to a single attocell and subscription to a single MVNO per time slot t. Constraint (8) and constraint (9) impose lower and upper bounds on the total data rate achieved by MVNO in each attocell, respectively. Constraint (10) is defined in (3), which requires a unique resource allocation to only one user subscribed to MVNO in each attocell. Constraint (11) imposes a lower bound on the power assigned to a resource in each attocell. This optimization problem (6)–(11) is a mixed integer non-linear optimisation problem. To this end, it cannot be optimally solved within a reasonable time window. In the following section, utility-based scheduling policies are developed to schedule users to their network slices, which can achieve network slices utility maximization.

IV. Utility-based service scheduling policies

Services running on network slices have different traffic characteristics and network performance requirements. The mMTC service generates low rate small size packets to support communications among a large number of wireless devices. The eMBB service generates large packet sizes that require a high bandwidth connection. It is assumed that both mMTC and eMBB services are more sensitive to throughput than delay. The URLLC service generates low rate small packet sizes packet, but requires stringent latency requirements [1]. Each service is characterized with a slice-specific utility function, which maps the network slice performance to utility values. These reflect the quality of resources allocated to the users offered the service. We design a utility-based scheduler to select a user $k \in \mathcal{K}_s^a$ at each time sub-frame t for transmission according to a dynamic customized resource utility policy.

The throughput of user k subscribed to MVNO s is calculated based on (2). The total throughput of a network slice is calculated based on (4). The transport layer throughput of network slice s in a LiFi attocell a can be calculated based on the buffer representing the slice, as follows:

$$\gamma_s^a = \sum_{k=1}^{|\mathcal{K}_s^a|}\sum_{t=1}^{T} L_{k,t}, \tag{12}$$

where $L_{k,t}$ denotes the size of packets transmitted from the LiFi attocell AP a to the users of MVNO s. The average network slice delay is calculated as the sum of the average time delay difference between the packet arrival time in the buffer and the time it is transmitted. This value is added up to the head-of-line (HoL) packet delay and then averaged over all the packets of slice s, given as follows:

$$D_s^a = \frac{1}{|\mathcal{K}_s^a|}\sum_{k\in\mathcal{K}_s^a}\frac{1}{K}\sum_{k=1}^{K} d_{\text{HoL}}^k, \tag{13}$$

where d_{HoL}^k denotes the packet HoL delay of user k; and K denotes the total number of packets of user k arrived at the slice buffer.

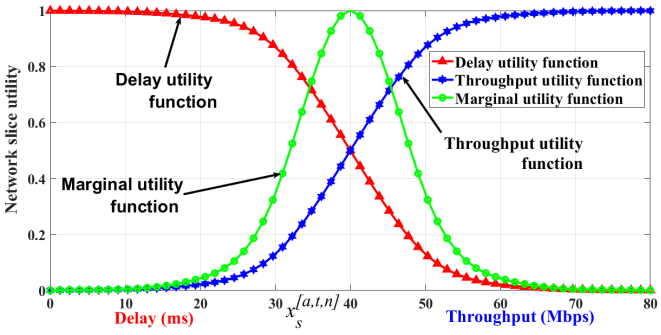

Fig. 2: Network slices utility functions

A sigmoidal utility function is formulated mathematically in (14), which maps each network slice performance in terms of delay and throughput requirements set by the MVNOs. It is continuous and differential, which makes it mathematically tractable. The utility of each user adds up to their cumulative slice utility. A scheduling policy (15) is conceived, which uses the slice utility function (14) to select a user at time t, $k^*(t) \in \mathcal{K}_s^a$, maximizing the total network slice utility, given as follows:

$$U_s^a(x_s^{[a,t,n]}) = \frac{e^{\nu\phi(x_s^{[a,t,n]} - x_{s_{\text{req}}}^{[a,t,n]})}}{1 + e^{\nu\phi(x_s^{[a,t,n]} - x_{s_{\text{req}}}^{[a,t,n]})}}, \tag{14}$$

$$k^*(t) = \arg\max_{k\in\mathcal{K}_s^a}\{\omega_s^a U_s^a(x_s^{[a,t,n]})\}, \quad \forall s,a \tag{15}$$

where $x_s^{[a,t,n]}$ denotes the measured slice service performance metric; ν is set to 1 and -1 to account for the increasing throughput and decreasing delay utility functions, respectively, as shown in Fig. 2. A non-negative parameter, ϕ, determines the function slope, given by [10]:

$$\phi = \frac{\ln(\frac{1-\xi}{\xi})}{\eta x_{s_{\text{req}}}^{[a,t,n]}}, \tag{16}$$

where $x_{s_{\text{req}}}^{[a,t,n]}$ denotes the QoS requirements of network slices (service). It determines the function abscissa shift from the QoS metric $x_s^{[a,t,n]}$. The constant variables, ξ and η, are taken to be 0.011 and 0.5 [10], respectively. The network slice aggregate throughput and the average delay of service running on

a slice s are measured in Mbps and ms, respectively, as shown in Fig. 2. The increase in the throughput of users increases the aggregate network utility of their MVNO $s, \forall s \in \mathcal{S}$, as the blue curve shows in Fig. 2. However, the increase in the delay of services offered to the users on the slice s drives lower the slice network utility of their MVNO s, as the red curve shows in Fig. 2. This total network slice utility maximization (NSUM)-based scheduling policy always selects a user that drives the highest network slice utility. Particularly, it prioritizes users with the shortest delay or highest throughput performance in the resource allocation process, which drives a higher network utility. However, this scheduling policy may not satisfy the long-term fairness criteria among users subscribed to the same MVNO s.

A fair network slice utility maximization (FNSUM)-based scheduling policy is developed, which controls resource utility fairness among slices by using a slice-specific control parameter, $\Upsilon_s^{a,t}$, at sub-frame t, given by:

$$\Upsilon_s^{a,t} = \frac{\psi_s^{a,t}}{(\sum_{i=1}^{t-1} e^{U_s^{a,i}})^t}, \tag{17}$$

where ψ_s^a is a predefined parameter denoting the slice specific service utility, which can be set to a value corresponding to priority, revenue or cost. $U_s^{a,t}$ denotes the utility of slice s calculated from (14) at sub-frame t. The weighted utility for slice $s \in S$ at sub-frame t is given as follows:

$$\Omega_s^{a,t} = \Upsilon_s^{a,t} U_s^{a,t}, \tag{18}$$

$$k^*(t) = \arg\max_{k \in \mathcal{K}_s^a} \{\omega_s^a \Omega_s^{a,t}\} \quad \forall s, a. \tag{19}$$

The FNSUM-based scheduling policy selects a user $k^*(t) \in \mathcal{K}_s^a$ based on (19). This policy can also opportunistically selects users from the slice with a higher specific service utility, $\psi_s^{a,t}$, to transmit.

A marginal utility function is derived in (20) as the first order derivative of the utility function (14) with respect to $x_s^{[a,t,n]}$. It determines the decrease or increase in the network slice utility as a result of making a scheduling decision with respect to the throughput or delay of user $k \in \mathcal{K}_s^a$, given as follows:

$$\frac{\partial U_s^a(x_s^{[a,t,n]})}{\partial x_s^{[a,t,n]}} = \frac{\nu\phi e^{\nu\phi(x_s^{[a,t,n]} - x_{s_{\text{req}}}^{[a,t,n]})}}{1 + e^{\nu\phi(x_s^{[a,t,n]} - x_{s_{\text{req}}}^{[a,t,n]})}} - \frac{\nu\phi e^{2\nu\phi(x_s^{[a,t,n]} - x_{s_{\text{req}}}^{[a,t,n]})}}{(1 + e^{\nu\phi(x_s^{[a,t,n]} - x_{s_{\text{req}}}^{[a,t,n]})})^2}. \tag{20}$$

According to the marginal utility function shown in Fig. 2, a MVNO is satisfied, when their measured aggregate throughput approaches and exceeds the throughput requirement in their service level agreement (SLA). The higher the weight, the higher the priority of a user to be assigned a resource. This network slice satisfaction maximization (NSSM)-based scheduling policy favors users with lower network resource utility in the resource allocation policy. The marginal utility value corresponding to the throughput of network slice s can be calculated from the utility function in (20). The marginal utility of the slice $s \in S$ at sub-frame $t-1$, $\Omega_s^{a,t-1}$ (21), is given as follows:

$$\Omega_s^{a,t-1} = \left| \frac{\partial U_s^a(x_s^{[a,t,n]})}{\partial x_s^{[a,t,n]}} \right|_{x_s^{[a,t,n]} = \gamma_s^{a,t-1,n}}, \tag{21}$$

$$k^*(t) = \arg\max_{k \in \mathcal{K}_s^a} \{\omega_s^a \Omega_s^{a,t-1} \gamma_s^{a,t,n}\} \quad \forall s, a, \tag{22}$$

where $\gamma_s^{a,t-1,n}$ is the total slice throughput at $[a, t-1, n]$. The scheduler selects a user $k^*(t) \in \mathcal{K}_s^a$ that achieves the NSSM scheduling policy (22). Similarly, the above scheduling policies can be calculated with respect to the users' head-of-line (HoL) packet delays. A user is scheduled based on (15), (19), or (22), considering ν in (20) and (14) is set to -1.

As each service runs on a network slice s has different sensitivities to delay and throughput, the network slice-specific parameter ω_s^a accounts for the slice throughput and delay utility weights per attocell a, denoted by ω_s^{th} and ω_s^{d}, respectively. The slice-specific parameter enables MVNOs to scale their network slice utility by adjusting either the throughput or delay utility weights to meet their services requirements and network resource conditions. Let the service guarantees of URLLC, mMTC, and eMBB be represented by a service tuple $[u\ m\ e]$, where $u, m, e \in [0, 1]$. This represents the percentage of resources or data rate to be guaranteed for each service during a sub-window time. For example, a service tuple $[1\ 1\ 1]$ indicates that the URLLC, mMTC, eMBB services should receive fully their maximum resource or data rate guarantees. A network slice is associated with two service tuples to represent their guarantees constraints based on the delay and throughput weights. These can be reset and programmed by the SDN controller. Hence, MVNOs can customize or prioritize network slice constraints guarantees by considering either delay or throughput utility weight in the resource scheduling process of their users.

V. Heuristic utility scheduling Algorithm

A heuristic utility based dynamic resource allocation algorithm is proposed to provide a heuristic solution to the optimization problem (6)–(11). The sub-carriers are allocated an equal power. First, the instantaneous data rate of each user is calculated on each sub-carrier based on (2). Second, the users of each MVNO $s \in S$ are sorted on each sub-carrier based on the product values of their slice scheduling utility priority weight and achieved date rate per sub-carrier. Third, a user in each slice s is scheduled for transmission according to the selected NSUM (15), FNSUM (19), or NSSM (22) policy. MVNOs are allocated the sub-carriers offering the best network utility until their data rate targets or resource guarantees are met. The resource allocation process is parameterized using four parameters: slice utility weight, user resource utility, minimum and maximum data rate targets of MVNOs. These simple steps do no involve any iterative processes, which make the heuristic algorithm converges faster towards the optimal resource allocation to users.

Algorithm 1: Network slice Utility-based heuristic scheduling algorithm.

Initialize:
$\mathbf{p}_{a,t,n} = \frac{P_{a,max}}{N}, \quad \forall a, t, n$
$\gamma_s^a = 0, \quad \forall s, a$: Initialise the data rate of MVNOs in each attocell
$\mathcal{M}_a^s = \{1, 2, \cdots, \mathcal{S}\}$: Set of MVNOs in attocell a
for $a \leftarrow 1$ *to* A **do**
  for $t \leftarrow 1$ *to* T **do**
    for $n \leftarrow 1$ *to* N **do**
      if $\gamma_s^a \leq \gamma_{s,\max}^a$ **then**
        begin
          switch *1* **do**
            $k_{a,s} \leftarrow$ Policy (15) NSUM
          switch *2* **do**
            $k_{a,s} \leftarrow$ Policy (19) FNSUM
          switch *3* **do**
            $k_{a,s} \leftarrow$ Policy (22) NSSM
        if $\gamma_s^a \geq \gamma_{s,\min}^a$ **then**
          $\mathcal{M}_a^s = \mathcal{M}_a^s - \{s\}$
        else
          $k_{a,s} \leftarrow [a, t, n]$
          $\gamma_s^a = \gamma_s^a + \gamma_{sk}^{a,t,n}$
      else
        $\mathcal{M}_a^s = \mathcal{M}_a^s - \{s\}$

TABLE I: Services and Traffic Simulation Parameters

Parameter	URLLC	mMTC	eMBB
d_s (delay (ms))	[0.5 , 1]	[20 , 50]	[10 , 40]
$[\gamma_{s,\min}^a, \gamma_{s,\max}^a]$ (Mbps)	[5 , 12]	[5 , 17]	[5 , 20]
λ_s(packets/ms)	2	20	7
L_s (bytes)	64	50	1450
$\lvert\mathcal{K}_s^a\rvert$ per attocell	2	5	3

VI. Performance Evaluation

A discrete time simulation environment was developed in MATLAB to evaluate the performance of Algorithm 1, in the sliced LiFi attocellular network shown in Fig. 1. This is installed in a room of size $5 \times 5 \times 3$ (length $\times$ width $\times$ height m^3). The LiFi AP channel simulation parameters are summarized in Table I [4]. Three network slices are established in the network, with each supporting a different 5G URLLC, mMTC, or eMBB service. The simulation parameters of these 5G services are introduced in Table I. The simulation time is divided into 80 sub-windows; each has a time length of 100 sub-frames. There are around 40 URLLC, mMTC, and eMBB users uniformly distributed in the network. They are scheduled every sub-frame following Algorithm 1, where the information required to calculate the cumulative distribution function (CDF) of network slices aggregate throughput and

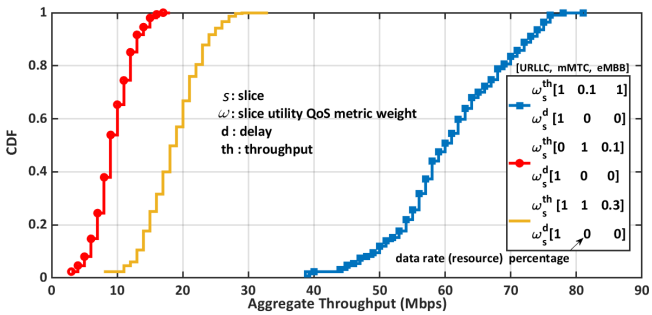

Fig. 3: CDF of network slice aggregate throughput providing eMBB service.

delay, users, and traffic flows are reported to the SDN controller. This enforces, every sub-window, the SLA constraint guarantees for each MVNO (slice).

The following scenarios focus on evaluating the performance of the proposed NSUM policy (15) in Algorithm 1. Initially the URLLC, mMTC, and eMBB network slices are arbitrarily allocated 20%, 30%, and 50% of the resources (i.e. times slots) in each sub-window. However, resources that are allocated to each network slice expand or shrink according to their slice resource customization parameter set in the service tuples by their MVNOs through the SDN controller, which are investigated in the the following scenarios.

In the first scenario, three different service tuples are considered to study the impact of changing the slice-throughput utility weight parameter ω_s^{th} on the aggregate throughput of eMBB and mMTC services, while fixing the URLLC slice-delay utility weight parameter ω_s^{d} to 1, as shown in Fig. 3 and Fig. 4. As a result, the performance of the eMBB and mMTC slices changes according to the increase and decrease of ω_s^{th}, which, respectively, increases or decreases their reliability in terms of throughput, as shown in Fig. 3 and 4. The URLLC network slice requires more resources to guarantee the delay requirement. The scheduler expands the initial resources amount allocated to the URLLC network slice, when ω_s^{th} of eMBB or mMTC network slice decreases, and vice-versa. When the mMTC users get their minimum data rate, the eMBB users get higher priority in the resource scheduling as they drive more utility. So, the performance of eMBB network slice does not experience a noticeable decrease due to changes in the ω_s^{th} of the mMTC network slice.

When the mMTC slice requires higher priority than the eMBB slice, the mMTC users can achieve higher throughput, as shown in Fig. 4. The channel conditions of users do not affect the scheduling priority of delay-sensitive services. Also, the utility increase of throughput sensitive slices can be caused by good channel conditions of their users, where the utility values can be above the minimum utility value. By changing ω_s^{th} the eMBB and mMTC network slices can expand or shrink their resources without affecting the resource allocation to the URLLC service users.

In the second scenario, three service tuples are considered to

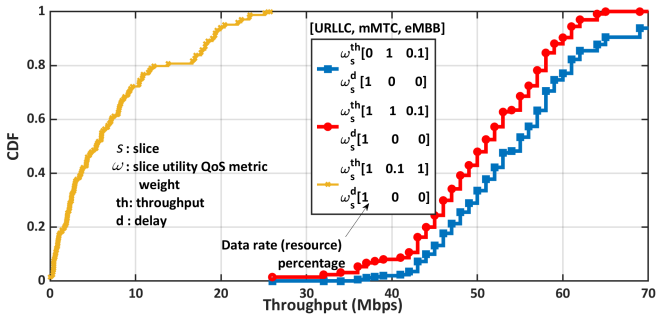

Fig. 4: CDF of network slice aggregate throughput providing mMTC service.

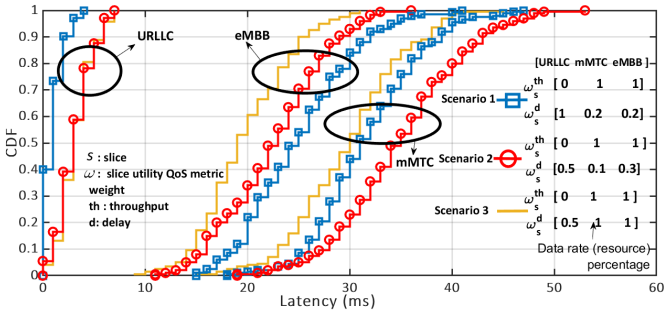

Fig. 5: CDF of network slices delay providing URLLC, mMTC, and eMBB services.

study the impact of changing the slice-delay weight parameter ω_s^{d} on the CDF of network slices average delay, while fixing their slice-throughput utility weight parameter ω_s^{th} to 1, as shown in Fig. 5. It is observed that when the value of the slice delay utility weight ω_s^{d} decreases from 1 to 0.5, 0.2, 0.1, their network utility values also decrease. The URLLC network slice is more reliable when the delay requirement is [3-8] ms. The eMBB network slice of eMBB is more reliable when the delay requirement [30-40] ms. The mMTC network slice is more reliable when the delay requirement is in [42-50] ms.

The proposed NSUM scheduling policy ensures the reliability of the 5G services, as can be observed from Fig. 3, Fig. 4, and Fig. 5. When the network slice delay or throughput weight metric is closer to 1, the proposed delay and throughput utility function-based scheduler maintains the service delay values of URLLC, mMTC and eMBB slices within their QoS service and reliability requirements. Other results, which are not included here due to space limitations, show that the FNSUM and NSSM policies achieve better network slice fairness comparing to the NSUM scheduling policy.

VII. Conclusion

The proposed utility-based resource quota to network slices scheduling policies could enable multiple MVNOs to dynamically offer 5G services on resource customized LiFi network slices. Sigmoidal utility functions have multiple parameters which could be designed to best characterize the services performance running on the different LiFi network slices. The proposed utility and derived marginal weight utility functions could serve as optimization objectives for users to maximize the total network utility with respect to their packets transmission throughput or HoL delay. Various utility-based scheduling policies could be derived, which provide priority weights to achieve different optimization objectives; such as the total network utility or users' satisfaction maximization. Hybrid user and network centric scheduling policies could be developed based on the priority weights. They enable MVNOs to adjust their slice-specific performance metric weights according to the network conditions and service requirements. As a next step, a performance comparison will be conducted on the proposed utility-based scheduling policies, considering other wireless technologies in the system model.

Acknowledgment

This work was supported by the EPSRC under grants EP/L020009/1 (TOUCAN Project), H2020-ICT-2019 5G-CLARITY project, and EP/R007101/1 (Established Career Fellowship).

References

[1] F. Schaich, B. Sayrac *et al.*, "FANTASTIC-5G:Flexible Air iNTerfAce for Scalable service delivery within wireless Communication networks of the 5th Generation," *Trans. On Emerging Telecommunications Technologies*, vol. 27, June 2016.

[2] H. Alshaer and H. Haas, "Bidirectional LiFi attocell access point slicing scheme," *IEEE Transactions on Network and Service Management*, vol. 15, no. 3, pp. 909–922, September 2018.

[3] H. Alshaer, "An overview of network virtualization and cloud network as a service," *International Journal of Network Management*, vol. 25, no. 1, pp. 1–30, January/February 2015.

[4] H. Alshaer, H. Haas, and O. Y. Kolawole, "An Optimal Networked LiFi Access Point Slicing Scheme for Internet-of-Things," in *Proc of ICC Workshop*, Montreal, June 2021.

[5] S. D'Oro, F. Restuccia, A. Talamonti, and T. Melodia, "Typhoon: An SDN enhanced real-time big data streaming framework," in *Proc. of IEEE Conference on Computer Communications (INFOCOM)*, Paris, France, June 2019, pp. 310–322.

[6] S. Mandelli, M. Andrews, S. Borst, and S. Klein, "Satisfying Network Slicing Constraints via 5G MAC Scheduling," in *Proc of Infocom*, Paris,France, June 2019, pp. 2332–2340.

[7] A. Lieto, I. Malanchin, and A. Capone, "Enabling Dynamic Resource Sharing for Slice Customization in 5G Networks," in *Proc of 2018 IEEE Global Communications Conference (GLOBECOM)*, December 2018.

[8] R. Kokku, R. Mahindra, H. Zhang, and S. Rangarajan, "NVS: A Virtualization Substrate for WiMAX Networks," in *Proc.of MobiCom '10*, Chicago, Illinois, USA, September 2010, pp. 233–244.

[9] M. I. Kamel, L. B. Le, and A. Girard, "LTE Wireless Network Virtualization: Dynamic Slicing via Flexible Scheduling," in *Proc. of 2014 IEEE 80th Vehicular Technology Conference (VTC Fall)*, Vancouver, BC, Canada, September 2014, pp. 1090–3038.

[10] E. B. Rodriguez, F. R. M. Lima, T. F. Maciel, and F. R. P.Cavalcanti, "Maximization of user satisfaction in OFDMA systems using utility-based resource allocation," *Wireless Communications And Mobile Computing*, vol. 16, pp. 376–392, 2016.

[11] R. Kokku, R. Mahindra, H. Zhang, and S. Rangarajan, "Cellslice: Cellular wireless resource slicing for active RAN sharing," in *Proc. of IEEE COMSNETS*, Bengaluru,India, 2013, pp. 1–10.

[12] J. Klaue, J. Gross, H. Karl, and A. Wolisz, "Utility-based Packet Scheduler for Wireless Communications," in *Proc of IEEE Conference on Local Computer Networks*, Tampa, FL, USA, November 2006.

[13] J. M. Kahn and J. R. Barry, "Wireless Infrared Communications," *IEEE*, vol. 85, no. 2, pp. 265–298, February 1977.

[14] J. Armstrong, "OFDM for Optical Communications," *Journal of Lightwave Technology*, vol. 27, no. 3, p. 189–204, February 2009.